communications biology

A Nature Portfolio journal

Article

https://doi.org/10.1038/s42003-025-07787-5

Escherichia Coli K1-colibactin meningitis induces microglial NLRP3/IL-18 exacerbating H3K4me3-synucleinopathy in human inflammatory gut-brain axis

Van Thi Ai Tran [1,2], Xiaohui Zhu[1,2], Ariunzaya Jamsranjav[1,2], Luke P. Lee [1,2,3] ✉ & Hansang Cho [1,2,4] ✉

Escherichia coli K1 (*E. coli* K1) meningitis early occurs in the gastrointestinal and causes severe damage to the central nervous system, including lifelong neurological complications in survivors. However, the cellular mechanism by which *E. coli* K1 may cause neuropathies is not well understood due to the lack of relevant human multi-organ models for studying multifaceted systemic inflammation across the gut-brain axis. Here, we reconstruct a multicellular model of the human gut-brain axis to identify the neuropathogenic mechanism driven by *E. coli* K1-colibactin meningitis. We observed that *E. coli* K1-genotoxic colibactin induced intestinal and peripheral interleukin 6, causing the blood-brain barrier injury and endothelial inflammation via the p38/p65 pathways. Serpin-E1 from the damaged cerebral endothelia induces reactive astrocytes to release IFN-γ, which reduces microglial phagocytosis of *E. coli* K1 and exacerbates detrimental neuroinflammation via NLRP3/IL-18 axis. Microglial IL-18 elevates neuronal reactive oxidative stress that worsens DNA double-strand breaks in *E. coli* K1-infected neurons, leading to H3K4 trimethylation and phosphorylation of alpha-synuclein. Our findings suggest therapeutic strategies for post-bacterial meningitis treatment to potentially prevent the initiation of synucleinopathy.

Escherichia coli K1 (*E. coli* K1) is a highly virulent bacterial pathogen that frequently causes neonatal meningitis, causing gastrointestinal symptoms at the early stage[1] and long-term neurological issues in over half of survivors[2]. Clinical reports have shown rectovaginal colonization of *E. coli* K1 in pregnant women is associated with the high risk of vertical transmission to their infants' gut during childbirth[3–5]. Additionally, *E. coli* K1 meningitis exhibits severe gut dysbiosis[6], high levels of inflammatory cytokines in the bloodstream[7], and brain damage[8]. These findings highlight the systemic detrimental effects of *E. coli* K1 infection, indicating that the gut-brain axis (GBA) may be a potential route for *E. coli* K1-induced meningitis.

The initial infection of the gut by *E. coli* K1 is facilitated by changes in the intestinal microbiota composition, leading to gut dysbiosis[9]. Within this dysbiotic microenvironment, *E. coli* K1 capitalizes on its virulence factors, such as genotoxic colibactin to adhere to and invade the intestinal epithelium (EP), breaching the gut barrier[10]. Especially, *E. coli* K1 can evade the host immune system due to the expression of capsule polysaccharide K1, a virulence factor that confers hostility to host cells' complement-mediated killing[11]. Additionally, the outer membrane protein enables *E. coli* K1 to evade phagocytosis by host macrophages through interactions with immune inhibitory receptors[12]. *E. coli* K1 is adept at disrupting blood-brain barrier (BBB) integrity and entering the brain, causing neuroinflammation and neuronal damage[13–15]. This invasion contributes to long-term neurological complications and potentially increases the risk of neurodegenerative disease (ND) onset.

Epidemiological studies suggested that Parkinson's disease (PD) patients are more likely to have a history of certain infections[16,17] or inflammatory bowel disease (IBD)[18,19]. Several studies have suggested the significant role of genotoxic colibactin-producing *E. coli* in the pathogenesis of IBD[20–22], implicating a suspected connection between childhood *E. coli* K1 meningitis and PD's etiology. A study demonstrated that 33 out of 34 neonatal isolates of *E. coli* K1 carried the clbA and clbP genes, which are part of the pks pathogenicity island and are necessary to produce genotoxic

[1]Institute of Biophysics, Sungkyunkwan University, Suwon, South Korea. [2]Department of Biophysics, Sungkyunkwan University, Suwon, South Korea. [3]Department of Medicine, Harvard Medical School, Brigham and Women's Hospital, Harvard Institute of Medicine, Harvard University, Boston, MA, USA. [4]Department of Intelligent Healthcare Medicine, Sungkyunkwan University, Suwon, South Korea. ✉e-mail: lplee@bwh.harvard.edu; h.cho@g.skku.edu

colibactin[23], a polyketide-peptide genotoxin induces genomic integrity in mammalian cells by initiating DNA damage, such as double-strand breaks (DNA-DSB)[24,25].

In the central nervous system (CNS), neurons are more susceptible to DNA damage than glial cells during *E. coli* K1 meningitis due to their long-lifespan and lack of robust DNA repair mechanisms[26]. Additionally, microglial phagocytosis of damaged neurons elevates reactive oxygen species (ROS) levels, further compromising neuronal DNA integrity[27]. Recent research has indicated that accumulation of DNA damage may occur before the onset of PD, suggesting its direct participation in neurodegeneration[28]. Upon DNA damage, chromatin unwinds, enabling repair enzyme access, a process regulated by epigenetic modifications that have been found in samples of PD patients, suggesting its significant role in disease pathology[29]. Moreover, several studies have found that epigenetic modifier TET1 or autophagy-lysomal system can regulate expression of *SNCA* gene encoding α-synuclein (α-Syn) protein[30,31], which accumulates abnormally as a pathological hallmark of PD. However, the specific mechanism by which *E. coli* K1 contributes to synucleinopathy is still uncertain.

In addition, it is well known that bacterial meningitis triggers neuroinflammatory responses[32,33]. Previous research has shown that the K1 capsule prevents direct recognition of the bacteria by microglia while inducing inflammatory responses in both microglia and astrocytes[34]. As astrocytic end-feet creates direct communication between the vascular system and the neuroglia within the CNS[35], astrogliosis may be initiated first upon *E. coli* K1 infection, which releases antimicrobial pro-inflammatory cytokines such as IFN-γ[36]. Interestingly, phagocytic activity of microglia can be promoted by astrocytic IL-4 and IL-10 via upregulation of TREM-2, but it is not clear whether pro-inflammatory cytokines disrupt phagocytosis in microglia[37]. At present, the role of microglia and astrocyte activation in host defense and immune surveillance during *E. coli* K1 meningitis remains unclear. Despite these advances, the systemic interplay among *E. coli* K1, neurodegeneration, and neuroinflammation via the GBA remains poorly understood due to the lack of a multi-organs system for studying step-wise pathogenesis upon *E. coli* K1 infection.

Although Transwell systems enable the co-culture of gut and brain barrier cells, it is impossible to incorporate blood-derived inflammatory factors between the two barriers complicating real-time imaging of cellular interactions. Organ-on-chips are considered a promising tool for elucidating the role of the human GBA in bacterial infection-induced NDs[38–40]. Therefore, we employed a GBA microfluidic chip as an infectious model to investigate meningitis-inducing neurodegeneration and neuroinflammation of *E. coli* K1. The GBA chip was reconstructed with all the necessary cellular components, including three main compartments for co-culture of gut EP and bacteria, brain endothelium (EC), tri-culture of neurons, astrocytes, and microglia. This model system allows us to recapitulate the complicated communication among the gut microbiota, the gut-blood-brain barrier (GBBB), and the CNS. Specifically, we hypothesize that *E. coli* K1 infection will lead to systemic inflammation and dysregulation of H3K4 trimethylation (H3K4me3), resulting in aberrant gene expression patterns associated with the severity of neurotoxic synucleinopathy.

Results

A model of human gut-brain inflammatory axis for studying systemic inflammation and neuropathogenesis associated with *E. coli* K1 meningitis

To develop the GBA chip system, we co-culture multiple human cells: gut EP, brain EC, neurons, astrocytes, and microglia, in a three-chamber platform connected via microchannels for interfacing and exchanging different cells (Fig. 1a, b). The microfluidic GBA chip was fabricated from polydimethylsiloxane (PDMS), with three parallel main channels connected to each other by microchannel arrays using standard soft lithographic techniques (Supplementary Fig. 1a–c). The gut EP and CNS channels were designed with dimensions of 100 × 3000 × 5000 μm in height, width, and length while the BBB channel was designed with dimensions of 100 × 600 × 5000 μm in height, width, and length. The interconnection microchannel arrays were designed with dimensions of 3 × 8 × 600 μm in height, width, and length.

To characterize GBBB function during *E. coli* K1-colibactin meningitis, we stained the gut EP and brain EC against vascular endothelial-cadherin (VE-Cad), αSyn, and phosphorylated αSyn (p-αSyn) (Fig. 1c, d, f). In our GBA system, *E. coli* K1 infection caused severe damage in the gut EP and mild injury in the brain EC. The infected gut EP strongly reduced the intensity level of VE-Cad markers indicating disruption of the gut barrier. Our results also observed a reduction in αSyn level while the level of pathogenic p-αSyn was increased dramatically in the *E. coli* K1-infected gut EP (Fig. 1c), indicating that Caco-2 cells can produce αSyn. Another study showed that Caco-2 cells are able to internalize αSyn aggregates, suggesting their relevance in modeling gut-derived contributions to PD pathogenesis[41]. In the CNS, *E. coli* K1 meningitis induced neuroinflammation and neurodegeneration-associated protein markers while reduced physiological markers in neurons, astrocytes, and microglia (Fig. 1e, f). Particularly, we found that *E. coli* K1 increases astrogliosis and microgliosis, evidenced by inducing level of glial fibrillary acidic protein (GFAP) for reactive astrocytes, CD86 as M1 microglia marker, and p65-NF-κB inflammatory signaling pathway. In addition, we observed epigenetic modification in neurons that happened during *E. coli* K1 meningitis, evidenced by an increase of H3K4me3 marker. This epigenetic induction associates the promotion of αSyn, which is post-translational modified into p-αSyn, which is a well-known neurotoxic protein in PD. In addition, we found the elevation of several inflammatory cytokines across multi-organs during *E. coli* K1-colibactin meningitis (Fig. 1g and Supplementary Fig. S2), which emphasized the crucial roles of systemic inflammation in *E. coli* K1 meningitis-associated neuropathies.

Intestinal and peripheral pro-inflammatory IL-6 predominantly promote BBB damage upon *E. coli* K1 meningitis

The GBBB is crucial in regulating interaction among the gastrointestinal (GI) tract, the immune system, and the brain in normal physiological conditions and meningitis[42]. Here, we hypothesized that *E. coli* K1-colibactin meningitis could lead to endoplasmic reticulum (ER) stress in both the gut EP and brain EC. Prolonged *E. coli* K1 infection in the gut EP may trigger calcium release from ER stores, subsequently causing an elevation of mitochondrial Ca^{2+} levels. This leads to mitochondrial ROS production, resulting in dysfunction of the gut barrier, allowing *E. coli* K1 to enter the systemic circulation. Meanwhile, *E. coli* K1 can evade detection and clearance by macrophages through various immune evasion strategies[43]. This evasion enables the bacteria to persist and proliferate, subsequently triggering an immune response, subsequently resulting in elevation of interleukin-6 (IL-6) as reported in patients with *E. coli* K1 meningitis[44–46]. These elevated levels of IL-6 may contribute to breakdown of the BBB via activation of p38/p65 and NLRP3 priming, facilitating infiltration of *E. coli* K1 into the CNS (Fig. 2a). To test this possibility, we reconstructed a GBBB in a microfluidic chip by co-culturing gut EP and brain EC in two distinct chambers connected by an array of micro-channels with 20 μm in width and 600 μm in length, which enables the bacteria movement and distinctly separate gut EP and EC to avoid medium shock. In the brain EC chamber, we additionally added soluble IL-6, a representative inflammatory cytokine from peripheral immunity, as observed in blood samples of *E. coli* K1 meningitis patients[7].

In the gut EP, *E. coli* K1-infected cells strongly increased the Rhod2-AM and ROS fluorescent signal fourfold greater than the control group (Fig. 2b, d), indicating calcium accumulation in the mitochondrial matrix induces ROS leading to the gut barrier disruption evidenced by the reduce of VE-Cad marker as previously shown in Fig. 1. In addition, our findings indicated a twofold increase in p-αSyn level in *E. coli* K1-stimulated gut EP (Fig. 2b, d). Interestingly, we observed a reduction in αSyn expression in the *E. coli* K1-exposured group (Fig. 2b, d), which suggests a possible mechanism for the phosphorylation of αSyn via mitochondrial dysfunction during *E. coli* K1-inducing intestinal inflammation. Long-term exposure of gut EP to *E. coli* K1 acts as a pro-apoptotic signal that triggers the outer

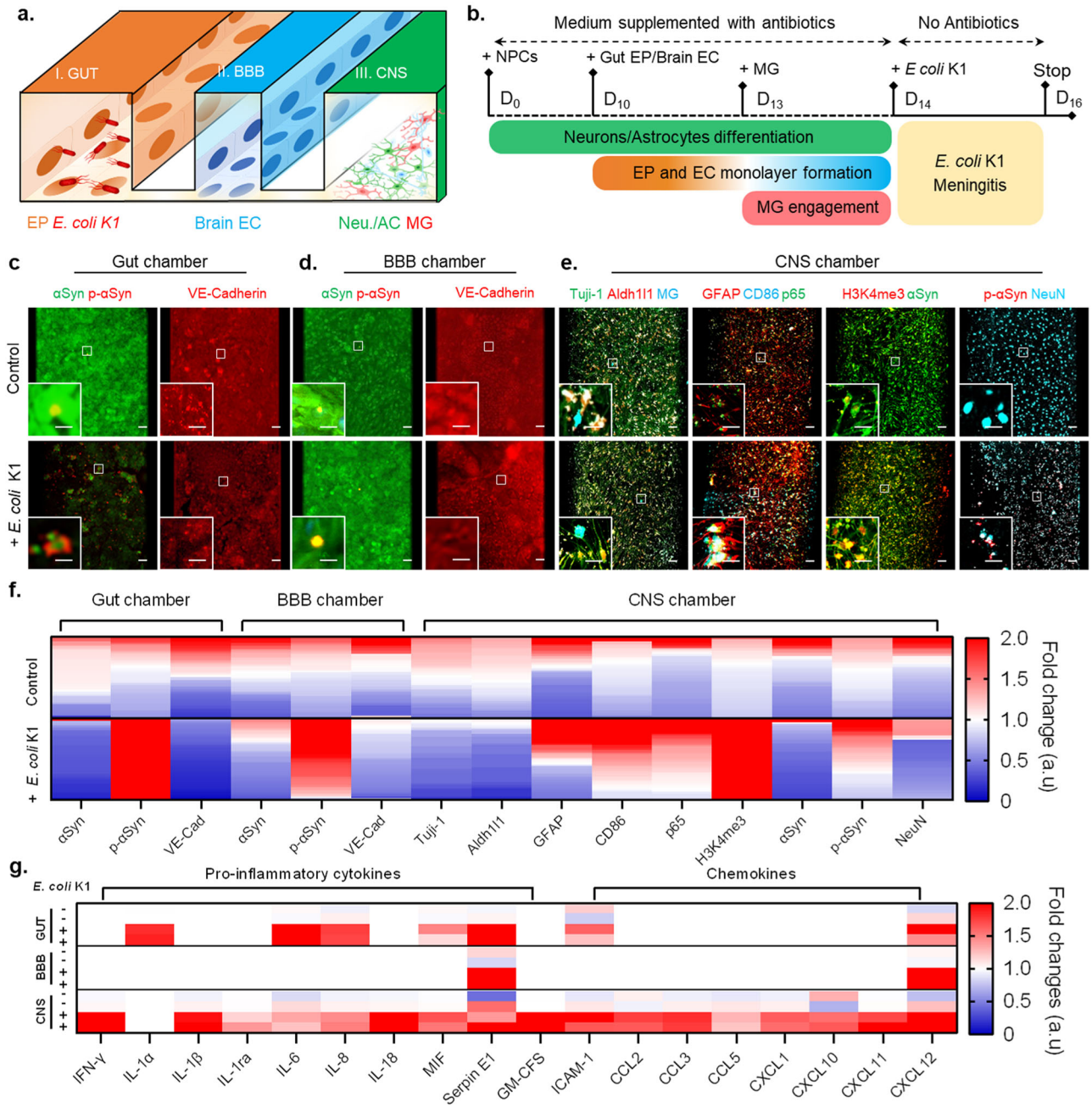

Fig. 1 | A microengineered model of human gut-brain axis for studying gut microbiome-derived neuropathogenesis: *E. coli* K1 meningitis and alpha-synucleinopathy. a A scheme and images of a gut-brain axis (GBA) platform for the study of gut infection-derived neurodegeneration with three compartments: gut epithelium (EP)/*E. coli* K1, brain endothelium (EC), and neurons/astrocytes/microglia (Neu./AC/MG). **b** Timeline of establishing GBA model for *E. coli* K1 meningitis. **c**–**e** Representative fluorescent images of GBA model showing physiological and pathological markers in gut epithelium chamber (αSyn/p-αSyn, VE-Cad), brain endothelium chamber (αSyn/p-αSyn, VE-Cad), and neurons/astrocytes/microglia chambers (Tuj1/Aldh1l1/MG, GFAP/CD86/p65, H3K4me3/αSyn, NeuN/p-αSyn), respectively. **f** Heat-map showing physiological and pathological markers in gut epithelium, brain endothelium, and neurons/astrocytes/microglia in GBA model. **g** Heat-map showing systemic multiple cytokines released from individual organ models during *E. coli* K1 infection in the GBA. All experiments were repeated three times and analyzed in fold changes. Scale bars, 50 μm (insets) and 100 μm (main) in Fig. 1c, e, 20 μm (insets) and 50 μm (main) in Fig. 1d. The full dataset used for Fig. 1 is available in Supplementary Data 1 and 5.

membrane to become permeable and facilitates the movement of cytochrome c (cyt c) away from cardiolipin, enabling the release of cyt c into the cytosol[47]. Cyt c, as a peroxidase, may be able to generate radicals on αSyn, ultimately initiating phosphorylation[48].

In the brain EC, we also observed similar scenarios with a slight increase in fluorescent signals of mitochondria Ca^{2+}, ROS, and p-αSyn in *E. coli* K1-infected cells (Fig. 2c, e). However, we did not observe severe damage to the brain endothelial monolayer during *E. coli* K1 meningitis in the co-culture model. It has been studied that *E. coli* K1 can be internalized by endothelial cells through receptor-mediated endocytosis, such as glycoprotein CD147[49] or Caspr1[15]. Next, our results illustrated that the *E. coli* K1-infected co-culture model can only significantly induce the p38-MAPK (Supplementary Fig. 3) and further increased by additional stimulation with IL-6 with twofold and 3.5-fold greater than the control group, respectively (Fig. 2f, g). Mitochondrial ROS can directly trigger p38-MAPK phosphorylation via a mechanism that requires

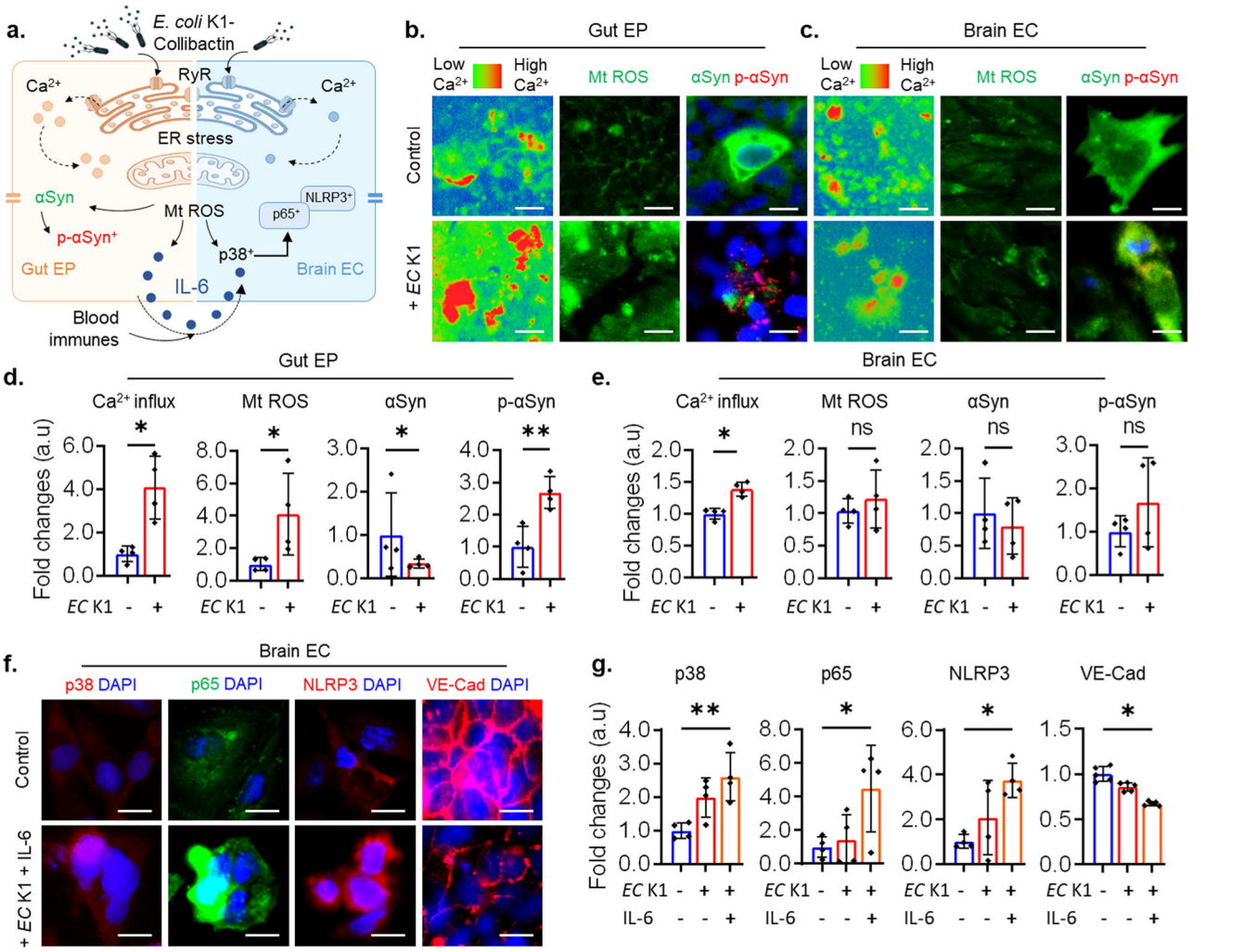

Fig. 2 | *E. coli* K1 induces intestinal and peripheral interleukin-6 causing blood-brain barrier inflammation and loosening tight junctions. a A signaling of how *E. coli* K1 induces gut-blood-brain barrier disruption in the co-culture of gut epithelium and brain endothelium. **b**–**e** Representative fluorescent images and quantitative analysis of calcium influx, Mt ROS, αSyn, and p-αSyn in the gut epithelium and brain endothelium respectively. **f**, **g** Representative fluorescent images and quantitative data of p38, p65-NFκB, NLRP3, and VE-Cad markers in the brain endothelium co-cultured with *E. coli* K1 and of IL-6 (100 ng/mL) treatment. All experiments were repeated four times independently and statistically analyzed by unpaired *t* test (**f**, **e**) and one-way ANOVA followed by Tukey HSD test (**g**) (*$p < 0.05$, **$p < 0.01$, and ***$p < 0.001$). All data were presented as mean ± standard deviation (SD). Scale bars, 20 μm. The full dataset used for Fig. 2 is available in Supplementary Data 2 and 5.

electron flow in the early stages of the mitochondrial electron transport chain, implying that either hydrogen peroxide or superoxide is involved in stimulating this process[50]. Also, we found that IL-6 initiated signaling cascades that release p65-NFκB for nuclear translocation and transcriptional activation (Fig. 2f, g) with 4-fold greater than control. Moreover, paired activation of p38/p65 promotes the NLRP3 priming leading to brain barrier disruption (Fig. 2f, g). In particular, the NLRP3 level increased 1.5-fold and fourfold without and with soluble IL-6 exposure, respectively. Similarly, the signal of VE-Cad marker reduced 1.5-fold in treatment with co-stimulated brain EC. Both p38-MAPK and p65-NFκB are capable of regulating the transcriptional expression of genes that participate in the inflammatory response, including components of the NLRP3 inflammasomes and upregulating pro-inflammatory cytokines.

Reactive astrocytic IFN-γ inhibits microglial phagocytosis, exacerbating neuroinflammation during *E. coli* K1 meningitis

During bacterial meningitis, astrocytes and microglia orchestrate vigilant immune surveillance within the CNS to combat the invading pathogens. However, dysregulated immune activation may lead to excessive neurotoxic neuroinflammation. In this study, we hypothesized that the BBB-penetrated *E. coli* K1 may first encounter astrocytes via recognizing pathogen-associated molecular patterns (PAMPs) from the bacteria due to the end-feet of astrocytes making direct contact with the BBB. This recognition could trigger the generation of IFN-γ and reactive astrogliosis at an early stage of meningitis, which may worsen due to inflammatory mediators from BBB damage. We did not observe the elevation of IFN-γ in microglia (Supplementary Fig. 4). Coincidently, the *E. coli* K1 itself can escape microglial phagocytosis via K1 capsule as reported in previous studies and activate mild microgliosis via PAMPs during their invasion in the CNS. More importantly, we proposed that reactive astrocytic IFN-γ could inhibit microglial phagocytosis of *E. coli* K1, reducing their ability to clear the invading pathogens effectively. As a result, this dysregulated microglial response contributes to the amplification of detrimental neuroinflammation (Fig. 3a). To test this hypothesis, we established central immune surveillance-on-a-chip by co-culturing human immortalized microglia and astrocytes with/without the presence of *E. coli* K1-stimulated brain EC conditioned medium ($_{K1}BBB_{CM}$) in astrocytes and IFN-γ in microglia.

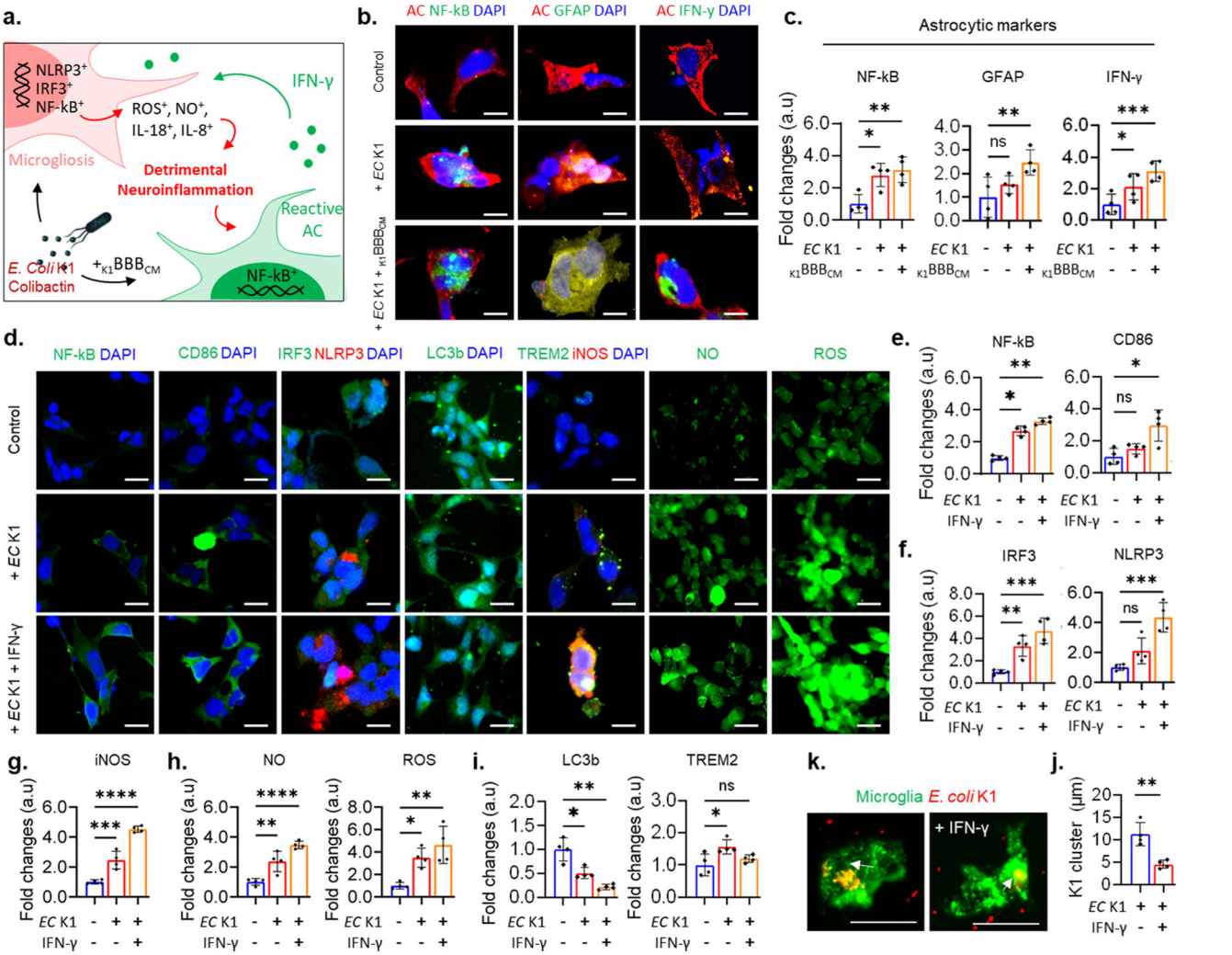

Fig. 3 | Astrocytic IFN-γ exacerbated neurotoxic microgliosis via NLRP3 inflammasome under *E. coli* K1 meningitis. a A signaling of *E. coli* K1 inducing detrimental neuroinflammation. **b**, **c** Fluorescent images and quantification of inflammatory (NF-κB, GFAP, IFN-γ) in astrocytes. **d** Representative images of inflammatory markers (NF-κB, CD86) and phagocytic markers (LC3b and TREM-2) in microglia with paired activation of IRF3 and NLRP3, inciting neuroinflammation evidenced by elevation of iNOS, NO, ROS. **e–i** Quantification of inflammatory and phagocytic markers in single culture microglia with and without IFN-γ. **k**, **j** Fluorescent images and quantification showing IFN-γ reduce microglial engulfment of *E. coli* K1 in meningitis. All experiments were repeated four times independently and statistically analyzed by One-way ANOVA followed by Tukey HSD test (Fig. 3c, e–i) and unpaired *t* test (Fig. 3k, j) (*$p < 0.05$, **$p < 0.01$, and ***$p < 0.001$). All data were presented as the mean ± standard. Scale bars, 20 μm in Fig. 3b and 50 μm in Fig. 3d, k. The full dataset used for Fig. 3 is available in Supplementary Data 3 and 5.

In astrocytes, we found an elevation of fluorescent signals across several reactive markers, including NF-κB, GFAP, IFN-γ in single and co-culture models in the bacteria-infected groups (Fig. 3b, c). In the single culture of astrocytes, *E. coli* K1 itself increased the level of NF-κB, GFAP, and IFN-γ with 2.5-fold, 2-fold, and 2-fold greater than the control of the single astrocytes model, respectively. Interestingly, all the astrocytic markers were significantly increased with the presence of $_{K1}BBB_{CM}$ during *E. coli* K1 infection, particularly 4-fold, 3-fold, and 4-fold greater than the non-infected group. Moreover, we revealed the interaction of microglia and astrocytes during *E. coli* K1 meningitis evidenced by the increase of reactive astrocytic markers in the *E. coli* K1-stimulated group compared to the control, with 3-fold, 2.5-fold, and 2.5-fold for NF-κB, GFAP, and IFN-γ, respectively (Supplementary Fig. 5). The astrocytic NF-κB signaling has been reported in common neurodegenerative astrogliosis[51] and in bacterial metabolites-induced astrogliosis[52]. Previous studies also showed the increase in GFAP level in cerebrospinal fluid of meningitis patients[53–55]. In acute infection, it has been shown that astrocytes are able to release type I interferon such as IFN-β[56], however, the role of astrocytic type II interferon like IFN-γ has been barely studied. Here, we showed excessive elevation of IFN-γ in *E. coli* K1 meningitis in the presence of inflammatory mediators from BBB damage, which highlights the synergistic interaction between vascular and astrocytic inflammation during meningitis.

After observing astrogliosis during *E. coli* K1 neuroinfection, our study continues to reveal the pivotal role of microglia in the pathophysiology of bacterial meningitis. We used the single and co-culture models as previously described in Fig. 3d & Supplementary Fig. 4 to investigate how microglia respond to *E. coli* K1 both on their own and alongside astrocytes. In the single culture of microglia, our results indicated slight increases in NF-κB and CD86 markers, suggesting microglial inflammation, with nearly 2.5-fold and 1.5-fold higher than the control for NF-κB and CD86, respectively (Fig. 3e). Upon observing elevated levels of IFN-γ in stimulated astrocytes, we added soluble IFN-γ into the single culture model of microglia which resulted in an excessive 3-fold induction in both NF-κB and CD86, almost like what was observed in the co-culture model where there was a 4-fold increase for NF-κB and 3-fold increase for CD86 (Fig. 3e). These results support our hypothesis on the critical role of

reactive astrocytic IFN-γ in dampening the M1 microglia during *E. coli* K1 meningitis.

We furthermore investigate how IFN-γ worsens the M1 state of microglia during *E. coli* K1 meningitis by measuring NO and ROS released from living cells and immunostaining against transcriptional markers in microglia (Fig. 3d). Previous studies reported that interferon regulatory factor 3 (IRF3) mediates a TLR3/NK-κB in viral and bacterial infection[57] and pre-treatment with the TLR3 agonist regulated innate immune responses in *E. coli* K1 meningoencephalitis[58]. In our study, we discovered that *E. coli* K1 itself can induce IRF3 level in microglia 3.5-fold higher than the control and 4.5-fold with the addition of soluble IFN-γ (Fig. 3f). Besides, another antimicrobial signaling pathway, NLRP3 inflammasome can be activated directly via bacterial components[59] or indirectly via NF-kB activation[60]. Also, it has been shown that phosphorylated form of IRF3 translocates into the nucleus and upregulates the expression of the NLRP3[61]. Our study found that *E. coli* K1 alone did not significantly activate NLRP3, but co-stimulation of *E. coli* K1 and IFN-γ increased NLRP3 signal with 4-fold greater than the control (Fig. 3d, f). Previous studies have demonstrated that elevated IFN-γ levels can enhance NLRP3 inflammasome activity, linking it to increased neuroinflammation and disease progression[62–64]. This suggests that in *E. coli* K1 meningitis, there is an initial upregulation of IRF3/NF-κB signaling followed by further stimulation of NLRP3 expression by reactive astrocytic IFN-γ. Subsequently, we observed an increase in the level of inducible nitric oxide synthase (iNOS) in a single infection with nearly 2.5-fold and co-stimulation with 4.5-fold greater than the control (Fig. 3g). Different studies demonstrated that microglia are the main source of iNOS during encephalitis[65] and their excessive level in the CNS may cause neurodegeneration in age-related diseases. We also found an excessive increase in nitric oxide (NO) as a downstream product of iNOS activation and ROS as evidence of oxidative stress in microglia during co-stimulation of *E. coli* K1 and IFN-γ (Fig. 3d, h), which indicates detrimental neuroinflammation state in microglia.

Meanwhile, our study found impaired phagocytosis in co-stimulated microglia, evidenced by reduction of tubule-associated protein 1 light chain 3 beta (LC3b) and triggering receptor expressed on myeloid cells 2 (TREM-2) markers (Fig. 3d, i). In a single culture of microglia, we found that *E. coli* K1 alone can inhibit autophagy, and co-stimulation with IFN-γ worsens this dysfunction, evidenced by a 2-fold and 4-fold reduction compared to the control, respectively. We also found a threefold decrease in LC3b signal in the *E. coli* K1-infected co-culture model. Our results showed that TREM-2 expression declines in the co-stimulation of *E. coli* K1 and IFN-γ (Fig. 3d, i). This may be attributed to the proteolytic cleavage of the TREM-2 receptor in the extracellular stalk domain, potentially mediated by a disintegrin and metalloproteinase enzyme such[66]. It has been discovered that TREM-2 has the ability to regulate immune cells to engulf bacteria, and elevation of TREM-2 induces bacterial clearance[67]. Therefore, the reduction of the TREM-2 signal in the treatment with IFN-γ, as shown in our results, suggested a reduction in microglial phagocytosis. Then, we further validated our hypothesis by measuring the size of *E. coli* K1 cluster that was engulfed by the microglia (Fig. 3k, j). In the presence of IFN-γ, microglia reduced their ability to clear *E. coli* K1, evidenced by more than a half reduction of bacterial cluster size. A previous study also found a similar phenomenon in macrophages co-stimulated with LPS and IFN-γ[68]. This impairment may exacerbate neuroinflammation in microglia, promisingly causing neuronal damage.

E. coli K1 causes neuronal DNA damage, leading to H3K4me3 promoting α-Syn phosphorylated by detrimental neuroinflammation

Emerging research in the fields of genomics and epigenetics has uncovered the role of epigenetic modifications in the pathogenesis of NDs[69] and microbe-host interaction. Here, we hypothesized that *E. coli* K1 triggers DNA-DSB in infected neurons due to their genotoxic colibactin, leading to permanent cellular senescence, which is associated with alterations in histone modifications, particularly an increase in H3K4me3 levels, which may lead to aberrant gene expression patterns of *SNCA*, results in the upregulation of αSyn expression. The accumulation of αSyn in neurons can be post-translational modified by microglial detrimental neuroinflammation that mediates neuronal mitochondrial oxidative stress (Fig. 4a). To validate this possibility, we used a co-culture model of neurons/astrocytes and a tri-culture model of neurons/astrocytes/microglia on chip.

As we expected, the results showed upregulation of DNA-DSB, permanent cell cycle arrest, and epigenetic modification in both *E. coli* K1-infected co-culture and tri-culture models (Fig. 4b, c and Supplementary Fig. 6). We found that gamma-H2AX (γ-H2AX), an acute sensor for DNA-DSB, were highly expressed in *E. coli* K1-infected co-culture and tri-culture with nearly threefold and fourfold greater than the controls, respectively. It has been reported that meningitic *E. coli* K1 is able to produce genotoxic colibactin that causes DNA damage[24,70]. As a response to DNA damage, the cells can run a DNA repair process to maintain genomic integrity, but most neurons are in a permanent post-mitotic stage. Therefore, once neurons get DNA damage, it triggers neuronal senescence associated with age-related neurological disorders. The p53-responsive gene p21 has frequently been regarded as essential for initiating cellular senescence, while p16 may play a more significant role in sustaining this phenotypic state. Our study observed high expression levels of senescence hallmarks, both p21, and p16, in infected neurons. Particularly, the p21 marker was increased threefold and 3.5-fold in the *E. coli* K1-infected co-culture and tri-culture compared to the controls, respectively. Meanwhile, the p16 marker induced nearly 2.5-fold in the infected models. Synchronically, the human brain samples of patients with NDs also harbor an increased proportion of senescent neurons[71].

Moreover, we observed significant increases in the level of H3K4me3 markers with threefold and 3.5-fold in the *E. coli* K1-infected co-culture and tri-culture, respectively, as shown in Fig. 4b, c and Supplementary Fig. 6. Subsequently, we found the increase of αSyn in the infected co-culture model with nearly 1.5-fold greater than the control while the expression of αSyn reduced in the *E. coli* K1 exposure tri-culture (Fig. 4e). Another research has also indicated that in the brains of individuals with PD, particularly in dopaminergic neurons, there are changes in the levels and distribution of H3K4me3 that are commonly associated with the *SNCA* promoter, facilitating a more open chromatin structure that allows gene expression[72]. This elevation ultimately leads to higher levels of αSyn.

Interestingly, in the co-culture model, we did not observe upregulation of p-αSyn, while our results showed 2.5-fold elevation of p-αSyn in the infected tri-culture (Fig. 4d, e). The increase of p-αSyn in the tri-culture further resulted in the mild reduce of synaptic marker (Synapsin I) and neuron marker (NeuN) as shown in Fig. 4d, e, which suggested the critical role of microglial detrimental neuroinflammation in synucleinopathy-associated neurodegeneration during *E. coli* K1 meningitis. Another study showed that acute meningitis-induced neuroinflammation elevates mitochondria-dependent apoptotic pathways, including increasing levels of cyto c, and caspase-3, in neurons[33]. Previously, we observed the same phenomena in the gut EP as the results discussed in Fig. 1. Thus, we validated whether microglial neuroinflammation induces calcium influx and mitochondrial oxidative stress during *E. coli* K1 meningitis. We found that there was in huge increase in calcium influx (Supplementary Fig. 7) and neuronal ROS (Fig. 4f) in the *E. coli* K1-infected tri-culture, which was associated with the increase of p-αSyn proved by the overlapped signal of ROS/NeuN/p-αSyn (Fig. 4f, g and Supplementary Fig. 8). Prior researches has demonstrated that the co-localization of cyt c and α-Syn, as well as the incubation of α-Syn with cyt c and hydrogen peroxide, results in the oxidative stress-driven aggregation of α-Syn. This aggregation occurs through the cross-linking of αSyn's tyrosine residues, forming di-tyrosine bonds[73,74].

Consequently, accumulated misfolded proteins may cause long-term autophagy dysfunction and neuroinflammation in microglia. We tested this hypothesis by using LPS and IFN-γ as a stimulator for neuroinflammation and pHrodo-conjugated amyloid-β as a model for misfolded protein in a single culture of microglia cells. We observed the reduction in uptaken

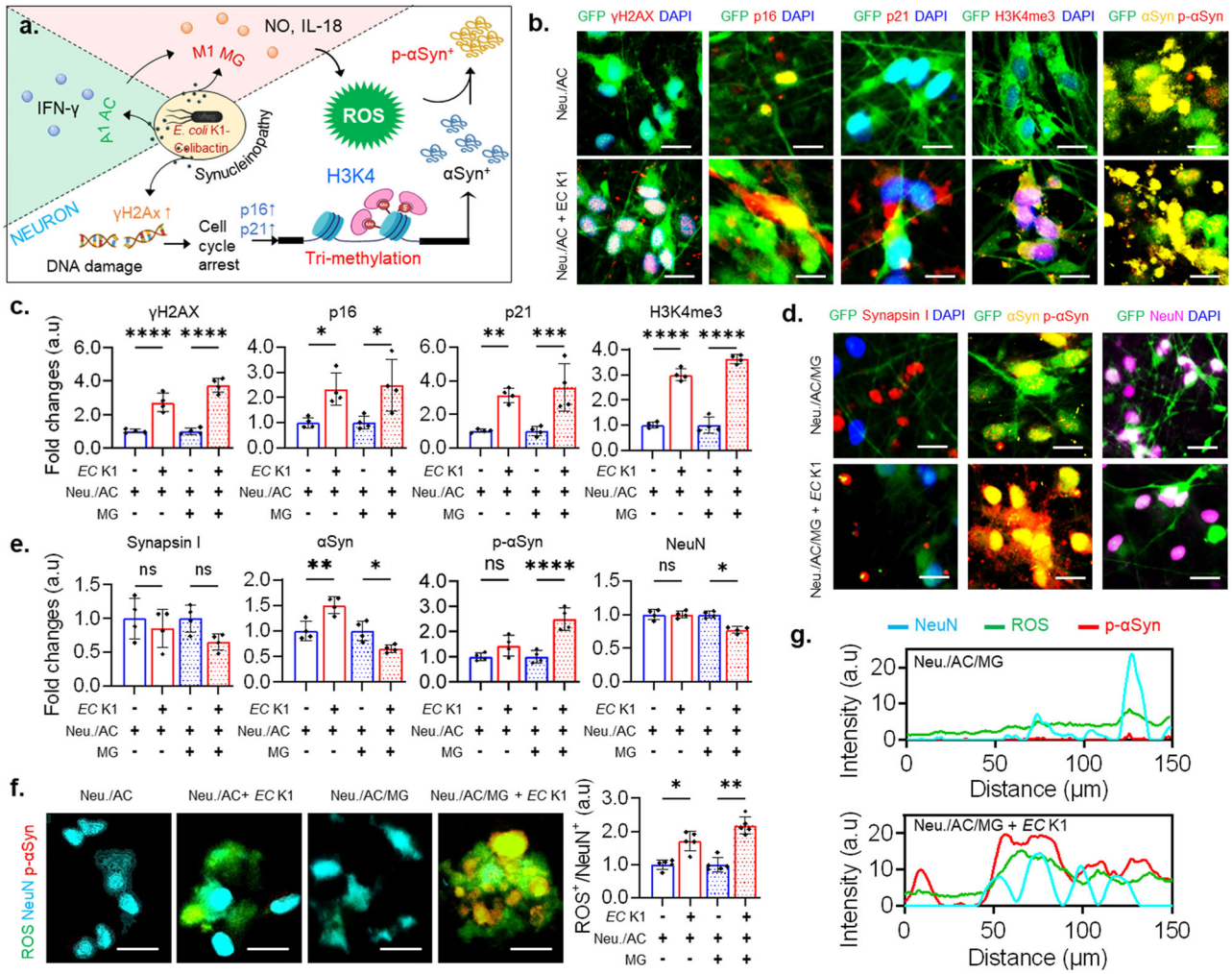

Fig. 4 | *E. coli* K1-colibactin and excessive neuroinflammation worsen DNA double-strand breaks in neurons, promoting H3K4 trimethylation and subsequently resulting in synucleinopathy. a A signaling of *E. coli* K1 (*EC* K1) inducing neurotoxic synucleinopathy. **b**, **d** Fluorescent images of neuronal markers in co-culture of neurons/astrocytes (Neu./AC) and tri-culture of neurons/astrocytes/microglia (Neu./AC/MG). **c**, **e** Quantification of neuronal markers in co-culture of neurons/astrocytes and tri-culture of neurons/astrocytes/microglia. **f** Representative images of tri-staining of NeuN/ROS/p-αSyn and quantification of neuronal ROS in co-culture and tri-culture system. **g** Graphs showing overlapped signals of NeuN, ROS, and p-αSyn. All experiments were repeated four times independently and statistically analyzed by One-way ANOVA followed by Tukey HSD test (*$p < 0.05$, **$p < 0.01$, and ***$p < 0.001$). All data were presented as mean ± standard deviation (SD). Scale bars, 50 μm. The full dataset used for Fig. 4 is available in Supplementary Data 4 and 5.

amyloid-β, dysfunction of autophagy markers, and increase in inflammatory markers (Supplementary Fig. 9). Taken all together, our study has demonstrated that neuronal epigenetic modification and ROS are critical factors inducing progressing accumulation of p-αSyn in *E. coli* K1 meningitis.

Discussion

PD is the second leading NDs affecting middle-aged and older adults and is increasing faster than those of any other NDs[75]. A key pathogenesis of PD is the intraneuronal aggregation of fibrillar αSyn protein translated by the *SNCA* gene[75]. Interestingly, pathological αSyn aggregates with prion-like self-propagating activity are present in the duodenum of PD patients[76]. Moreover, a recent study has found evidence of αSyn aggregates in the gut samples and brain samples of people and mice with IBD[77], which has suggested the connection of GBA. While a study reported that patients with IBD are at high risk for meningitis[78], several researches have demonstrated the existence of *E. coli* at the sites of inflammation in the gut of IBD patients[79]. However, the interconnection among bacterial meningitis, gut inflammation, and synucleinopathy remains unclear. Overall, our study has shown the notion of a complex interplay between *E. coli* K1 meningitis, systemic inflammation, and synucleinopathy via the GBA.

In the human GI tract, enterendocrine cells are well-known to express αSyn[80] in response to bacterial ligands and metabolites[81]. However, it is possible for non-sensory cells in gut EP to generate αSyn due to their abundant presence in the intestinal lumen and direct contact with gut bacteria. Our results demonstrated that long exposure to *E. coli* K1 triggered mitochondrial calcium influx, which in turn led to the elevation of ROS and αSyn phosphorylation at serine 129 when compared to the untreated model, which offers insight into how *E. coli* K1 can induce p-αSyn in gut EP. Moreover, we observed severe inflammation in gut EP upon *E. coli* K1 infection, which may exacerbate mitochondrial dysfunction and calcium dysregulation, potentially amplifying ROS generation and p-αSyn. Upon crossing the gut barrier, several studies have shown that *E. coli* K1 is capable of evading detection and phagocytosis by macrophages[43], key immune cells tasked with engulfing and eliminating invading pathogens. Also, previous research has demonstrated that chicken macrophages secrete pro-inflammatory cytokines, such as IL-6, in response to early *E. coli* K1 infection[82]. Although IL-6 can enhance the bactericidal activity of macrophages[83] and amplify the cell-mediated immune response against

E. coli K1[84], it may contribute to BBB damage. Here, our findings suggest that the dysregulation of IL-6 production during *E. coli* K1 meningitis can exacerbate BBB disruption, thereby facilitating bacterial invasion into the CNS and contributing to the pathogenesis of meningitis.

Upon encountering *E. coli* K1, astrocytes rapidly respond to the presence of the bacterium by becoming activated and releasing release pro-inflammatory cytokines. Here, we identified IFN-γ as a crucial early mediator involved in astrocytic immune response upon *E. coli* K1 infection, exerting both beneficial and neurotoxic effects[85]. Our results suggest that astrocytic release of IFN-γ can modulate microglial activity, leading to reduced phagocytic capacity and subsequently increased *E. coli* K1 survival in the CNS. Several studies have shown that IFN-γ signaling in microglia may induce the upregulation of MHC class II and other immune-related molecules, promoting their activation and pro-inflammatory functions[86]. While this activation is essential for mounting an effective immune response against pathogens, it can also shift microglia towards a more inflammatory phenotype, which may be associated with impaired phagocytosis. This dysregulation may result in inadequate clearance of pathogens and cellular debris, further exacerbating neuroinflammation and neuronal damage.

While the infection of neuronal cells by diverse microbial agents has been documented in numerous viral infections, the invasion of neurons by bacterial pathogens is a comparatively rare occurrence. A recent study found that *E. coli* K1 is capable of invading hippocampus neurons, which mainly rely on the bacterial IbeA and neuronal contactin-associated protein[15], which suggests a possible mechanism of how *E. coli* K1 may directly induce neuronal damage. Our study elucidated that *E. coli* K1 meningitis induces a G1/S phase arrest in infected neurons, a critical cell cycle checkpoint that regulates DNA replication and cell division. This arrest is a result of the interaction between host cell signaling pathways and bacterial virulence factors, culminating in the dysregulation of neuronal cell cycle progression. Furthermore, this arrest triggers the aberrant accumulation of αSyn, a protein predominantly found in presynaptic terminals, which plays a central role in PD pathology. The mechanism underlying this accumulation involves histone modifications, specifically the H3K4me3, which alters the chromatin structure and transcriptional regulation of genes associated with αSyn expression. Importantly, our findings revealed that microglial inflammation elevates neuronal ROS, which contributes to the phosphorylation of αSyn, potentially leading to progressive neurodegeneration.

Typically, *E. coli* K1 meningitis is an acute infectious process with mortality rates ranging from 10% to 15% within the first 3–5 days[87]. Patients who receive effective treatment during the early stage have a higher chance of survival. However, elevated levels of H3K4me3 and p-αSyn were observed during *E. coli* K1 meningitis may persist and accumulate over time, even after the acute phase has resolved. The stable epigenetic change of H3K4me3 probably predisposes neurons to increased vulnerability to aging and other stressors in survivors. Meanwhile, the lasting presence of p-αSyn promotes aggregation and may potentially initiate neurodegeneration. In this study, we suggest that early-life infections may act as a first hit, priming the brain for later neurodegeneration via life-long accumulation of p-αSyn. Although our study did not include the blood immune cells, we utilized IL-6 a representative inflammatory cytokine to mimic peripheral inflammation and its contribution to the BBB injury upon *E. coli* K1 meningitis. While our simplified GBBB model does not fully recapitulate the complex cellular interaction of human BBB due to the lack of astrocytes and pericytes, it allows for the study of *E. coli* K1-mediated barrier damage in part. In addition, future studies could incorporate with in vivo model and integrate complementary quantitative methods to gain deeper insights into the assessment of oligomeric forms of αSyn and the complex biological mechanisms underlying *E. coli* K1 meningitis-synucleinopathy as presented in our study.

Conclusions

Our study reveals that *E. coli* K1-induced meningitis can lead to DNA-DSB in neurons, resulting in permanent cellular senescence. This process is associated with alterations in histone modifications, particularly an increase in H3K4me3 levels, which may lead to aberrant gene expression patterns of *SNCA*, resulting in the upregulation of αSyn expression–a protein closely linked to the pathogenesis of PD. The αSyn in neurons can be phosphorylated into p-αSyn by neurotoxic microgliosis-inducing ROS. Taking all together, we provide insights into the mechanism of *E. coli* K1 infection as a potential risk factor for synucleinopathy onset.

Methods

Study design

This study aimed to develop a microphysiological system that mimics the human GBA to investigate systemic inflammation and neuropathogenesis associated with *E. coli* K1 meningitis. To achieve this, we created a three-compartment microfluidic platform using photolithography and soft lithography, allowing for the culture of five different types of cells spanning the human GBA, including gut epithelial cells (EP), brain endothelial cells (EC), neurons (Neu.), astrocytes (AC), and microglia (MG). The final platform consisted of three GBA microfluidic devices integrated into a glass slide at the bottom and an acrylic array at the top, serving as a medium reservoir (Supplementary Fig. 1c). This design enables three replicates within a single platform, supports long-term cell survival, and facilitates easy imaging. To assess the complex interplay of *E. coli* K1 infection in gut-blood-brain-barrier damage, a critical aspect of meningitis, we developed a gut-blood-brain-barrier model by co-culturing *E. coli* K1, gut EP, and brain EC in separate chambers. Then, soluble IL-6 was introduced to the brain EC chamber 24 hours after infecting the gut EP chamber with *E. coli* K1. This experimental approach was designed to mimic the peripheral immune responses that occur during the progression of bacterial meningitis. Specifically, the delay in IL-6 addition reflects the time-dependent activation of systemic inflammation, where gut-originated infections trigger the release of IL-6 into circulation. These cytokines subsequently contribute to the development of meningitis. Barrier damage was then identified through immunostaining of tight junction proteins. The fluorescent signal was normalized by the non-stimulated group to get fold changes.

To demonstrate detrimental neuroinflammation during *E. coli* K1 meningitis, we established an immune surveillance model by co-culturing human immortalized astrocytes and microglia in the CNS chamber with or without *E. coli* K1 infection. Immunostaining against neuroinflammatory markers, along with living cell assays and analysis of multiple cytokines, were utilized to evaluate inflammatory responses during *E. coli* K1 meningitis. To investigate the role of astrocytic IFN-γ on microglial-mediated neuroinflammation, soluble IFN-γ was introduced into single cultures of microglia 4 hours prior to stimulation with *E. coli* K1. This pre-treatment period was selected based on evidence that IFN-γ primes microglial activation, facilitating the upregulation of inflammatory signaling pathways and the release of pro-inflammatory mediators. The signals induced by this treatment were subsequently normalized to non-stimulated microglia to account for baseline activation. Next, to evaluate IFN-γ-impaired microglial phagocytosis of *E. coli* K1 and neurotoxic proteins, we co-cultured *E. coli* K1 and microglia with pHrodo-Aβ with/without prior stimulation with IFN-γ. Finally, we mimicked the neurons-glia interaction model by tri-culturing hNPC-derived neurons and astrocytes with immortalized microglia in the CNS chamber to identify the role of neuroinflammation in neurodegeneration during *E. coli* K1 meningitis. We used immunostaining against neurodegenerative markers and other living cell assays to characterize neuropathogenesis associated with *E. coli* K1 meningitis.

Preparation of *Escherichia coli* K1

Escherichia coli K1 (ATCC, Cat. 700973) was proliferated in Tryptic Soy Broth (Sigma-Aldrich, Cat. 22092-500 G). The culture was placed at 37 °C with shaking at 100 × rpm overnight. The bacterial culture was diluted 100-fold until the optical density at 600 nanometers wavelength attained a value of 1 under identical experimental conditions. Finally, the bacterial pellets were separated from the bacterial conditioned medium by centrifuging at 10,000 × *g* in 10 min.

Microfluidic chip fabrication

We utilized photolithography to fabricate the SU8 master mold and soft lithography methods to reconstruct a microfluidic platform comprising three chambers for reconstructing multi-organ interaction (Supplementary Fig. 1), by pouring a mixture of 10% (v/v) of polydimethylsiloxane base and 1% (v/v) of curing agent (Sylgard 184 A/B, Dow Corning, Midland, MI, USA) into the master mold. Then, the mixture is vacuumed for 20 min to completely remove all remaining bubbles, followed by curing at 60 °C for at least two hours for polymerization. Next, the PDMS sheets are removed from the mold and punched 2 mm diameter holes to make the inlets and outlets while the medium reservoirs are fabricated by laser cutting the 6 mm thick acrylic sheets (Zing 24, Epilog Laser, Golden CO., USA). Then, the PDMS and acrylics are bonded together by using a mixture of uncured PDMS and curing agents. The assembled platforms were placed at 60 °C for at least 4 hours for full binding. Lastly, the glass slides were bonded with the PDMS using oxygen plasma (PX-250, March Plasma System Petersburg FL, USA) with settings of 350 mW power for 2 min.

Gut epithelial cell preparation

The Caco-2 cell line (ATCC, Manassas, VA, USA, Cat. HTB-37), which is derived from human intestinal epithelial cells, was proliferated in Dulbecco's Modified Eagle's Medium-high glucose (Sigma-Aldrich, Cat. D5796-500ML). The cells were proliferated using the medium containing 10% (v/v) of fetal bovine serum from Sigma-Aldrich (Cat. F2442) and 1% (v/v) of Penicillin-Streptomycin (Lonza, Cat. 17-745E). Then, the Caco-2 cells were placed at 37 °C and 5% CO_2 until reaching approximately 80% of confluency. The Caco-2 culture medium was exchanged every two days with fresh medium.

Brain endothelial cell preparation

Human immortalized brain endothelial cells (EC) were acquired from Cedarlane Laboratories (Ontario, Canada) and cultured in a T25 flask coated with 1% (v/v) of collagen. The cells were proliferated using the medium containing endothelial cell growth basal medium-2 (Lonza, Cat. 190860), 1% (v/v) of penicillin-streptomycin (Sigma-Aldrich, Cat. P4333), 1.4 µM hydrocortisone (Sigma-Aldrich, Cat. H0888-1G), 10 mg/mL L-Ascorbic acid (MedChem, Cat. HY-B0166G), 1% (v/v) of chemically defined lipid concentrate, 10 mM HEPES (Gibco-BRL, Cat. 15630-106), 20 ng/mL bFGF (Stemgent, Cat. 03-2002), and supplement with 5% v/v of FBS (Sigma-Aldrich, Cat. F2442). The cells were placed at 37 °C and 5% CO_2 until reaching 80% of confluency. The brain endothelial cell culture medium was exchanged every two days with fresh media.

Proliferation of human microglial cells

The immortalized human microglia (SV40 cell line) were purchased from Applied Biological Material Inc. (ABM, Cat. T0251) and were grown in a T25 flask (SPL Life Sciences, Cat. 70012) containing 5 mL of microglial proliferation medium that contained 90% (v/v) of Pigrow III (ABM, Cat. TM003) and 10% v/v of FBS (Sigma-Aldrich, Cat. F2442), and 1% (v/v) of penicillin-streptomycin (Sigma-Aldrich, Cat. P4333). Then, the cells are maintained at 37 °C with 5% CO_2. and the cell culture medium is exchanged every 2 days until it reaches 90% of confluency.

Proliferation of human astrocytes

The immortalized human astrocytes (SV40 cell line) were purchased from Applied Biological Material Inc. (ABM, Cat. T0280) and were grown in a 1% (v/v) of collagen-coated T25 flask (SPL Life Sciences, Cat# 70012) containing 5 mL of microglial proliferation medium that contained 90% (v/v) of Pigrow IV (ABM, Cat. TM004) and 10% (v/v) of FBS (Sigma-Aldrich, Cat. F2442), and 1% (v/v) of penicillin-streptomycin (Sigma-Aldrich, Cat. P4333). Then, the cells are maintained at 37 °C with 5% CO_2. and the cell culture medium is exchanged every 2 days until it reaches 90% of confluency.

Proliferation and differentiation of human neural progenitor cells

Human neural progenitor cells (ReN) were purchased from EMD Millipore (Billerica, MA, US, Cat. SCC008) and cultured in a 1% (v/v) of Matrigel-coated T25 flasks (SPL Life Sciences, Pocheon, Korea, Cat# 70012). The 1% (v/v) of Matrigel coating solution is prepared by adding 10 µL of Matrigel (Corning, Cat# 356235) to 0.99 mL of DPBS (Sigma-Aldrich, Cat. D8537). The ReN cells are cultured in a proliferation medium containing DMEM/F12 (Gibco, Cat. 11320033), 0.1% (v/v) of Heparin (2 mg/mL, StemCell Technology, Cat. 7980), 2% (v/v) of B27 (Gibco, Cat. 17504044), and 1% (v/v) of Penicillin/Streptomycin (Sigma-Aldrich, Cat. P4333), bFGF (20 ng/ml, Stemgent, Cat. 03-0002) and hEGF (20 ng/ml, Sigma-Aldrich, Cat. SRP6253)[88]. The cells were maintained at 37 °C with 5% CO_2 and the cell culture medium was exchanged every 2 days until it reached 90% confluency.

Next, the human neural progenitor cells were differentiated in a differentiation medium containing DMEM/F12 (Gibco, Cat. 11320033), 0.1% (v/v) of Heparin (2 mg/mL, StemCell Technology, Cat. 7980), 2% (v/v) of B27 (Gibco, Cat. 17504044), and 1% (v/v) of Penicillin/Streptomycin (Sigma-Aldrich, Cat. P4333) for 14 days to obtain neurons/astrocytes. The differentiated medium was exchanged every two days with fresh media.

Preparation of human GBA models

We reconstructed the gut-brain platform to study the pathogenesis of *E. coli* K1 meningitis-inducing systemic inflammation and neuropathogenesis. We coated microfluidic chambers with 10 µL of Poly D-lysine (Sigma-Aldrich, Cat. A-003-M), then placed at RT for 20 min. The CNS chamber was incubated with 1% (v/v) Matrigel solution at 37 °C for 30 min. Then, we loaded 10 µL of ReN cells (10^8 cells/mL) to the CNS chamber and placed the platform at 37 °C and 5% CO_2 for 30 min for attachment. Next, we added 100 µL of fresh medium into each reservoir and exchanged every other day for 14 days to get neurons/astrocytes. Prior to gut EPs and brain ECs loading, we coated the gut chamber and BBB chamber with 10 µL of 2 mg/mL collagen Type I at 37 °C for 30 min. Then, we seeded 10 µL of gut EPs (10^8 cells/mL) and brain ECs (10^7 cells/mL) to each chambers and placed the platform in a 5% CO_2 incubator at 37 °C for at least 5 days to get the monolayer of gut EP and brain EC. Two days prior to infection, we added immortalized microglia (10^5 cells/mL) to the CNS to recreate neuron-glia interaction. After that, we infected *E. coli* K1 to the gut EP chamber and placed it in a 5% CO_2 incubator at 37 °C for an additional 2 days (Supplementary Fig. 1d).

The microfluidic devices were maintained under semi-dynamic conditions, enabling passive media to flow through a hydrostatic pressure gradient without requiring an external pump (Supplementary Fig. 1e). This gradient was generated by adding 200 µL of fresh medium to the inlet reservoir and 100 µL to the outlet reservoir of each device. Consequently, media flowed sequentially from the inlet through the main chambers of the gut EP, brain EC, and CNS compartments, as well as the interconnecting microchannels, effectively mimicking the physiological communication between these systems. This setup mimics the physiological communication between these compartments. This passive flow ensured continuous nutrient delivery and waste removal for the culture cells.

Preparation of GBBB models

To create GBBB model, we coated microfluidic chambers with 10 µL of Poly D-lysine (Sigma-Aldrich, Cat. A-003-M), incubated at RT for 20 min, and washed with PBS 1X (HanLab, Cat. K19274065). We seeded 10 µL of gut EPs (10^8 cells/mL) and brain ECs (10^7 cells/mL) to each chambers and placed the platform in a 5% CO_2 incubator at 37 °C for at least 5 days to get the monolayer of gut EP and brain EC, then we infected *E. coli* K1 to the gut EP chamber.

Preparation of central immune surveillance models

To create immune surveillance-on-chip, we coated microfluidic chambers with 1% v/v of Matrigel and incubated at 37 °C for 30 min. Then, we loaded 10 µL of immortalized microglia/astrocytes (10^7 cells/mL) and incubated the devices in a 5% CO_2 incubator at 37 °C for 1 hour for cell attachment. Next, we added 100 µL of fresh medium to each reservoir. Prior to infection, we exchanged medium without antibiotics and added *E. coli* K1 directly to the CNS chamber and incubated in a 5% CO_2 cell culture incubator at 37 °C.

Preparation of neuron-glial interaction models

To create neuron-glia interaction-on-chip, we coated microfluidic chambers with we coated microfluidic chambers with 1% v/v of Matrigel and incubated at 37 °C for 30 min. Afterward, we loaded 10 μL of ReN cells (10^8 cells/mL) into the CNS chamber and incubated the platforms at 37 °C and 5% CO_2 for 1 hour. Finally, we added 100 μL of fresh medium and exchanged every two days for 14 days. Two days prior to infection, we added immortalized microglia to the CNS to recreate neuron-glia interaction. After that, we infected *E. coli* K1 directly to the CNS chamber and placed at 37 °C and 5% CO_2.

Assessment of microglial phagocytosis assay

The microglia SV40 cells were proliferated in a T25 flask until they reached 90% confluency, as described previously. Then, the cells were detached by incubating with Trypsin EDTA (Sigma, Cat. T3924) at 37 °C and 5% O_2 for 2–3 min. Then, the cells were harvested by centrifuging at 1300 × rpm in 3 min and placed in a mixture of 1 mL of Diluent C and 2 μL of the green-fluorescent dye (Sigma-Aldrich, Cat. PKH67GL). The mixture was then placed at room temperature for 5 min and centrifuged at 1300 × rpm for 3 min. The microglia cells were captured in the FITC channel (Alexa488). The *Escherichia coli* K1 were grown in Tryptic Soy Broth (Sigma-Aldrich, Cat. 22092-500 G) overnight at 37 °C. Then, the cells were harvested by centrifugation at 4500 × rpm for 10 min and were promptly resuspended into a dye solution containing 1% (v/v) of BactoView™ Live red dye (Biotium, Cat. 40101-T). The mixture was placed at 37 °C for 30 min in dark, then the cells were harvested by centrifugation and resuspended into growth medium according to experimental purpose. The bacterial cells were captured in the TRITC channel (Alexa 594).

ROS assessment

ROS was assessed by dichlorofluorescein diacetate (H2DCFDA) (ThermoFisher, Cat. D399) according to the provided guidance from the manufacture. Briefly, the cell samples were incubated with fresh medium containing the 5 μM of ROS indicator for 30 min in the dark at 37 °C and 5% CO_2. Then, fresh medium was added into the cells to incubate for an additional 30 min at 37 °C and 5% CO_2. Finally, ROS signals were captured using a fluorescence microscope (Nikon TiE microscope, Nikon with FITC channel (Alexa488).

NO assessment

We used DAF-FMTM diacetate (ThermoFisher, Cat. D-23844) to measure NO according to the manufacturer's protocol. Particularly, the cells were placed with 10 nM DAF-FMTM diacetate in fresh medium at 37 °C and 5% CO_2. Then, the NO indicator solution was removed and replaced by fresh medium for an additional incubation at 37 °C with 5% CO_2 for 30 min. Lastly, the NO signals were imaged by fluorescence microscope (Nikon TiE microscope, Nikon) with FITC channel (Alexa488).

Multiple cytokines assessment

A multiplex cytokine array kit (R&D Systems, Cat. ARY005) was used to assess the expression of various cytokines and chemokines. Briefly, the cell culture-conditioned medium was harvested and centrifuged to remove the remaining cell pellets. Then, a mixture of conditioned medium and biotinylated detection antibodies was incubated for at least 2 hours while the nitrocellulose membranes were blocked with a blocking buffer. Then, the prepared mixture was added to the blocked nitrocellulose membranes, allowing binding of the target proteins and immobilized capture antibodies. The arrays were placed at 4 °C on a shaker for at least 6 hours and gently washed at least three times at 10-min intervals to remove any unbound antibodies. Chemiluminescent detection solution and streptavidin-horseradish peroxidase were used to assess the intensity signal that is proportional to the level of proteins in the conditioned medium. Then, we used ImageJ software (Wayna Rasband, NIH) to quantify the results.

Calcium imaging

The cell samples were incubated with 5 μM of the calcium-sensitive dye Rhod2-AM (Abcam, Cat. 142780) at 37 °C in the dark for 30 min, following the manufacturer's guidance. Then, the cells were gently washed twice with calcium-free HBSS and imaged using fluorescence microscope in FITC channel. The fluorescence intensity was normalized to the baseline value F_0 and reported as the mitochondrial calcium concentration.

Immunostaining

Cells were fixed with 4% paraformaldehyde (Biosesang, Cat. PC2031-100-00) for 30 min, then washed with phosphate-buffered saline containing 0.1% (v/v) of Tween®20 to remove the excessing paraformaldehyde. Next, the fixed cells were treated with 0.1% (v/v) of Triton-X 100 in PBST for 30 min at and blocked with 3% (v/v) of BSA for 1 hour. Primary antibodies were diluted to an appropriate concentration and treated to the samples overnight at 4 °C (as detailed in Supplementary Table 1). Subsequently, the samples were treated with secondary antibodies diluted 1:200 and DAPI for 2 hours. Finally, the samples were washed five times with PBST before imaging using Nikon fluorescence microscope. The intensity of immune reactivity was quantified with ImageJ software (Wayna Rasband, NIH).

Statistical analysis

All the data were relatively normalized by the control group and reported as mean ± standard deviation. The number of replicates was provided in the description of figure captions. The statistical differences between were analyzed by unpaired *t*-test and One-way ANOVA followed by Tukey's post-hoc test using SPSS software (IBM, NY, US). *P* value less than 0.05 was considered statistically significant. The symbols NS, *, **, and *** denoted no significance, p value < 0.05, p value < 0.01, p value < 0.001, and p value < 0.0001 respectively.

Reporting summary

Further information on research design is available in the Nature Portfolio Reporting Summary linked to this article.

Data availability

All data supporting the finding of this study are provided within the paper and the Supplementary Information.

Received: 23 September 2024; Accepted: 19 February 2025;
Published online: 07 March 2025

References

1. Moussiegt, A. et al. Escherichia coli community-acquired meningitis in adults: a case series of 29 patients in France. *Clin. Microbiol. Infect.* **28**, 1304–1305 (2022).
2. Pons, S. et al. A high-throughput sequencing approach identifies immunotherapeutic targets for bacterial meningitis in neonates. *eBioMedicine* **88**, 104439 (2023).
3. Liu, T.-H. et al. Rectovaginal colonization with pathogenic escherichia coli during pregnancy and neonatal outcomes. *Infect. Drug Resist.* **12**, 3103–3112 (2019).
4. Khazaei, Z., Ghorbani, P., Namaei, M. H., Rezaei, Y. & Yousefi, M. Prevalence of escherichia coli k1 rectovaginal colonization among pregnant women in Iran: virulence factors and antibiotic resistance properties. *Micro. Drug Resist.* **26**, 1201–1207 (2020).
5. Watt, S. et al. Escherichia coli strains from pregnant women and neonates: Intraspecies genetic distribution and prevalence of virulence factors. *J. Clin. Microbiol.* **41**, 1929–1935 (2003).
6. Nhu, N. T. K. et al. High-risk Escherichia coli clones that cause neonatal meningitis and association with recrudescent infection. *Elife* **12**, RP91853 (2023).
7. Ribes, S. et al. Resistance of the brain to escherichia coli K1 infection depends on MyD88 signaling and the contribution of neutrophils and monocytes. *Infect. Immun.* **81**, 1810–1819 (2013).

8. Liu, W. T. et al. New insights into meningitic Escherichia coli infection of brain microvascular endothelial cells from quantitative proteomics analysis. *J. Neuroinflamm.* **15**, 291 (2018).
9. Kim, J. K., Lee, K. E., Lee, S. A., Jang, H. M. & Kim, D. H. Interplay between human gut bacteria escherichia coli and lactobacillus mucosae in the occurrence of neuropsychiatric disorders in mice. *Front Immunol.* **11**, 273 (2020).
10. Harnack, C. et al. Short-term mucosal disruption enables colibactin-producing E. coli to cause long-term perturbation of colonic homeostasis. *Gut Microbes* **15**, 2233689 (2023).
11. Miajlovic, H. & Smith, S. G. Bacterial self-defence: how Escherichia coli evades serum killing. *FEMS Microbiol. Lett.* **354**, 1–9 (2014).
12. Mittal, R. et al. Fcγ receptor i alpha chain (CD64) expression in macrophages is critical for the onset of meningitis by Escherichia coli K1. *PLoS Pathog.* **6**, e1001203 (2010).
13. Fu, J. et al. Meningitic Escherichia coli α-hemolysin aggravates blood–brain barrier disruption via targeting TGFβ1-triggered hedgehog signaling. *Mol. Brain* **14**, 116 (2021).
14. Zhu, N., Liu, W., Prakash, A., Zhang, C. & Kim, K. S. Targeting E. coli invasion of the blood–brain barrier for investigating the pathogenesis and therapeutic development of E. coli meningitis. *Cell Microbiol*. **22**, e13231 (2020).
15. Zhao, W. D. et al. Caspr1 is a host receptor for meningitis-causing Escherichia coli. *Nat. Commun.* **9**, 2296 (2018).
16. McGee, D. J., Lu, X. H. & Disbrow, E. A. Stomaching the possibility of a pathogenic role for helicobacter pylori in Parkinson's disease. *J. Parkinsons Dis.* **8**, 367–374 (2018).
17. Huang, H. K. et al. Helicobacter pylori infection is associated with an increased risk of Parkinson's disease: a population-based retrospective cohort study. *Park Relat. Disord.* **47**, 26–31 (2018).
18. Zhang, X. Y. et al. Association between irritable bowel syndrome and risk of parkinson's disease: a systematic review and meta-analysis. *Front. Neurol.* **12**, 720958 (2021).
19. Liu, B. et al. Irritable bowel syndrome and Parkinson's disease risk: register-based studies. *npj Park Dis.* **7**, 5 (2021).
20. Sepehri, S., Kotlowski, R., Bernstein, C. N. & Krause, D. O. Phylogenetic analysis of inflammatory bowel disease associated Escherichia coli and the FimH virulence determinant. *Inflamm. Bowel Dis.* **15**, 1737–1745 (2009).
21. Unni, R. et al. Evolution of E. coli in a mouse model of inflammatory bowel disease leads to a disease-specific bacterial genotype and trade-offs with clinical relevance. *Gut Microbes* **15**, 2286675 (2023).
22. Abdelhalim, K. A., Uzel, A. & Ünal, N. G. The role of major virulence factors and pathogenicity of adherent-invasive Escherichia coli in patients with Crohn's disease. *Prz. Gastroenterol.* **15**, 279–288 (2020).
23. Dubinsky, V., Dotan, I. & Gophna, U. Carriage of colibactin-producing bacteria and colorectal cancer risk. *Trends Microbiol*. **28**, 874–876 (2020).
24. McCarthy, A. J. et al. The genotoxin colibactin is a determinant of virulence in Escherichia coli K1 experimental neonatal systemic infection. *Infect. Immun.* **83**, 3704–3711 (2015).
25. Nougayrède, J. P. et al. Escherichia coli induces DNA double-strand breaks in eukaryotic cells. *Science*. **313**, 848–851 (2006).
26. Welch, G. M. et al. Neurons burdened by DNA double-strand breaks incite microglia activation through antiviral-like signaling in neurodegeneration. *Sci. Adv.* **8**, eabo4662 (2022).
27. Yanuck, S. F. Microglial phagocytosis of neurons: diminishing neuronal loss in traumatic, infectious, inflammatory, and autoimmune CNS disorders. *Front. Psychiatry* **10**, 712 (2019).
28. Milanese, C. et al. Activation of the DNA damage response in vivo in synucleinopathy models of Parkinson's disease. *Cell Death Dis.* **9**, 818 (2018).
29. Tsalenchuk, M., Gentleman, S. M. & Marzi, S. J. Linking environmental risk factors with epigenetic mechanisms in Parkinson's disease. *npj Park Dis.* **9**, 123 (2023).
30. Guhathakurta, S. et al. Regulation of αlpha-synuclein gene (SNCA) by epigenetic modifier TET1 in Parkinson disease. *Int. Neurourol. J.* **26**, S85–S93 (2022).
31. Gordevicius, J. et al. Epigenetic inactivation of the autophagy–lysosomal system in appendix in Parkinson's disease. *Nat. Commun*. **12**, 5134 (2021).
32. Farmen, K., Tofiño-Vian, M. & Iovino, F. Neuronal damage and neuroinflammation, a bridge between bacterial meningitis and neurodegenerative diseases. *Front. Cell. Neurosci*. **15**, 680858 (2021).
33. Giridharan, V. V. et al. Neuroinflammation trajectories precede cognitive impairment after experimental meningitis-evidence from an in vivo PET study. *J. Neuroinflamm.* **17**, 5 (2020).
34. Liu, P. et al. Collaborative Action of Microglia and Astrocytes Mediates Neutrophil Recruitment to the CNS to Defend against Escherichia Coli K1 Infection. *Int. J. Mol. Sci*. **23**, (2022).
35. Kadry, H., Noorani, B. & Cucullo, L. A blood–brain barrier overview on structure, function, impairment, and biomarkers of integrity. *Fluids Barriers CNS* **17**, 69 (2020).
36. Kwon, H. S. & Koh, S. H. Neuroinflammation in neurodegenerative disorders: the roles of microglia and astrocytes. *Transl. Neurodegener*. **9**, 42 (2020).
37. Yi, S. et al. IL-4 and IL-10 promotes phagocytic activity of microglia by up-regulation of TREM2. *Cytotechnology* **72**, 589–602 (2020).
38. Wu, Q. et al. Organ-on-a-chip: recent breakthroughs and future prospects. *Biomed. Eng. Online* **19**, 9 (2020).
39. Ramadan, Q. & Zourob, M. Organ-on-a-chip engineering: toward bridging the gap between lab and industry. *Biomicrofluidics* **14**, 041501 (2020).
40. Raimondi, I. et al. Organ-on-a-chip in vitro models of the brain and the blood-brain barrier and their value to study the microbiota-gut-brain axis in neurodegeneration. *Front. Bioeng. Biotechnol*. **7**, 435 (2020).
41. Yang, Z. X. et al. Addition of α-synuclein aggregates to the intestinal environment recapitulates Parkinsonian symptoms in model systems. *Acta Pharm. Sin.* **45**, 36–51 (2024).
42. Cheng, Y., Chen, C. & Zhang, F. Immunity orchestrates a bridge in gut-brain axis of neurodegenerative diseases. *Ageing Res. Rev*. **85**, e0039921 (2023).
43. Yang, J. et al. O -acetylation of capsular polysialic acid enables escherichia coli k1 escaping from siglec-mediated innate immunity and lysosomal degradation of e. coli -containing vacuoles in macrophage-like cells. *Microbiol. Spectr*. **9** (2021).
44. Prasad, R., Kapoor, R., Srivastava, R., Mishra, O. P. & Singh, T. B. Cerebrospinal fluid TNF-α, IL-6, and IL-8 in children with bacterial meningitis. *Pediatr. Neurol.* **50**, 60–65 (2014).
45. Vázquez, J. A., Adducci, M. D. C., Coll, C., Monzón, D. G. & Iserson, K. V. Acute meningitis prognosis using cerebrospinal fluid interleukin-6 levels. *J. Emerg. Med.* **43**, 322–327 (2012).
46. Kalchev, Y. et al. Cytokine profile in patients with acute bacterial meningitis. *Cytokine* **170**, 156315 (2023).
47. Garrido, C. et al. Mechanisms of cytochrome c release from mitochondria. *Cell Death Differ.* **13**, 1423–1433 (2006).
48. Kumar, A., Ganini, D. & Mason, R. P. Role of cytochrome c in α-synuclein radical formation: Implications of α-synuclein in neuronal death in Maneb- and paraquat-induced model of Parkinson's disease. *Mol. Neurodegener*. **11**, 70 (2016).
49. Doran, K. S. et al. Host–pathogen interactions in bacterial meningitis. *Acta Neuropathol.* **131**, 185–209 (2016).
50. Kulisz, A., Chen, N., Chandel, N. S., Shao, Z. & Schumacker, P. T. Mitochondrial ROS initiate phosphorylation of p38 MAP kinase during hypoxia in cardiomyocytes. *Am. J. Physiol. Lung Cell. Mol. Physiol*. **282**, L1324-9 (2002).
51. Liddelow, S. A. & Barres, B. A. Reactive astrocytes: production, function, and therapeutic potential. *Immunity* **46**, 957–967 (2017).
52. Sun, H. et al. Bacteria reduce flagellin synthesis to evade microglia-astrocyte-driven immunity in the brain. *Cell Rep*. **40**, 111033 (2022).

53. Guo, Y. et al. Glial fibrillary acidic protein astrocytopathy presented as meningitis: a case report. *Heliyon* **10**, e26827 (2024).
54. Li, K., Wu, J., Chen, J. & You, Y. Glial fibrillary acidic protein astrocytopathy and tuberculous meningoencephalitis occurring in a patient with Legionella pneumonia: a case report. *BMC Neurol.* **23**, 69 (2023).
55. Liang, Y., Wang, G., Li, B., Li, G. & Zeng, H. Autoimmune glial fibrillary acidic protein astrocytosis mimicking tuberculous meningitis: a retrospective study. *J. Neurol.* **270**, 4860–4867 (2023).
56. Hwang, M. & Bergmann, C. C. Alpha/beta interferon (IFN-α/β) signaling in astrocytes mediates protection against viral encephalomyelitis and regulates IFN-γ-Dependent Responses. *J. Virol*. **92**, e01901-17 (2018).
57. Doyle, S. E. et al. IRF3 mediates a TLR3/TLR4-specific antiviral gene program. *Immunity* **17**, 251–263 (2002).
58. Ribes, S. et al. Pre-treatment with the viral Toll-like receptor 3 agonist poly(I:C) modulates innate immunity and protects neutropenic mice infected intracerebrally with Escherichia coli. *J. Neuroinflamm.* **17**, 24 (2020).
59. Sha, W. et al. Human NLRP3 Inflammasome senses multiple types of bacterial RNAs. *Proc. Natl. Acad. Sci. USA* **111**, 16059–16064 (2014).
60. Zhong, Z. et al. NF-κB restricts inflammasome activation via elimination of damaged mitochondria. *Cell* **164**, 896–910 (2016).
61. Li, N. et al. STING-IRF3 contributes to lipopolysaccharide-induced cardiac dysfunction, inflammation, apoptosis and pyroptosis by activating NLRP3. *Redox Biol*. **24**, 101215 (2019).
62. Xie, C. B. et al. Complement membrane attack complexes assemble NLRP3 inflammasomes triggering IL-1 activation of IFN-γ-primed human endothelium. *Circ. Res.* **124**, 1747–1759 (2019).
63. Labzin, L. I., Lauterbach, M. A. R. & Latz, E. Interferons and inflammasomes: Cooperation and counterregulation in disease. *J. Allergy Clin. Immunol.* **138**, 37–46 (2016).
64. He, H. et al. Microglial priming by IFN-γ involves STAT1-mediated activation of the NLRP3 inflammasome. *CNS Neurosci. Ther.* **30**, e70061 (2024).
65. Marques, C. P., Cheeran, M. C.-J., Palmquist, J. M., Hu, S. & Lokensgard, J. R. Microglia are the major cellular source of inducible nitric oxide synthase during experimental herpes encephalitis. *J. Neurovirol.* **14**, 229–238 (2008).
66. Feuerbach, D. et al. ADAM17 is the main sheddase for the generation of human triggering receptor expressed in myeloid cells (hTREM2) ectodomain and cleaves TREM2 after Histidine 157. *Neurosci. Lett.* **660**, 109–114 (2017).
67. Wu, Z., Yang, S., Fang, X., Shu, Q. & Chen, Q. Function and mechanism of TREM2 in bacterial infection. *PLOS Pathog.* **20**, e1011895 (2024).
68. Schütze, S., Kaufmann, A., Bunkowski, S., Ribes, S. & Nau, R. Interferon-gamma impairs phagocytosis of Escherichia coli by primary murine peritoneal macrophages stimulated with LPS and differentially modulates proinflammatory cytokine release. *Cytokine X* **3**, 100057 (2021).
69. Berson, A., Nativio, R., Berger, S. L. & Bonini, N. M. Epigenetic regulation in neurodegenerative diseases. *Trends Neurosci.* **41**, 587–598 (2018).
70. Chagneau, C. V. et al. Uropathogenic E. coli induces DNA damage in the bladder. *PLoS Pathog*. **17**, e1009310 (2021).
71. Herdy, J. R. et al. Increased post-mitotic senescence in aged human neurons is a pathological feature of Alzheimer's disease. *Cell Stem Cell* **29**, 1637–1652.e6 (2022).
72. Södersten, E. et al. A comprehensive map coupling histone modifications with gene regulation in adult dopaminergic and serotonergic neurons. *Nat. Commun*. **9**, 1226 (2018).
73. Hashimoto, M., Takeda, A., Hsu, L. J., Takenouchi, T. & Masliah, E. Role of cytochrome c as a stimulator of α-synuclein aggregation in Lewy body disease. *J. Biol. Chem.* **274**, 28849–28852 (1999).
74. Ruf, R. A. S., Lutz, E. A., Zigoneanu, I. G. & Pielak, G. J. α-synuclein conformation affects its tyrosine-dependent oxidative aggregation. *Biochemistry* **47**, 13604–13609 (2008).
75. Parkinson disease-associated cognitive impairment. *Nat. Rev. Dis. Prim*. **7**, 46 (2021).
76. Vascellari, S. et al. α-Synuclein seeding activity in duodenum biopsies from Parkinson's disease patients. *PLoS Pathog*. **19**, fuad022 (2023).
77. Espinosa-Oliva, A. M. et al. Inflammatory bowel disease induces pathological α-synuclein aggregation in the human gut and brain. *Neuropathol. Appl. Neurobiol*. **50**, e12962 (2024).
78. Kochar, B., Jiang, Y. & Long, M. D. Patients with inflammatory bowel diseases are at higher risk for meningitis. *J. Clin. Gastroenterol.* **55**, 350–354 (2021).
79. Pilarczyk-Zurek, M. et al. Possible role of Escherichia coli in propagation and perpetuation of chronic inflammation in ulcerative colitis. *BMC Gastroenterol*. **13**, 61 (2013).
80. Chandra, R. et al. Gut mucosal cells transfer α-synuclein to the vagus nerve. *JCI Insight* **8**, e172192 (2023).
81. Hurley, M. J. et al. α-Synuclein expression in response to bacterial ligands and metabolites in gut enteroendocrine cells: an in vitro proof of concept study. *Brain Commun*. **5**, fcad285 (2023).
82. Bagheri, S. et al. Production of interferon gamma and interleukin 17A in chicken T-cell subpopulations hallmarks the stimulation with live, irradiated and killed avian pathogenic Escherichia coli. *Dev. Comp. Immunol*. **133**, 104408 (2022).
83. Chen, S. et al. Macrophages in immunoregulation and therapeutics. *Signal Transduct. Target. Ther*. **8**, 207 (2023).
84. Bhat, P., Leggatt, G., Waterhouse, N. & Frazer, I. H. Interferon-γ derived from cytotoxic lymphocytes directly enhances their motility and cytotoxicity. *Cell Death Dis*. **8**, e2836 (2017).
85. Zhang, J. Yin and yang interplay of IFN-γ in inflammation and autoimmune disease. *J. Clin. Invest.* **117**, 871–873 (2007).
86. Ottum, P. A., Arellano, G., Reyes, L. I., Iruretagoyena, M. & Naves, R. Opposing roles of interferon-gamma on cells of the central nervous system in autoimmune neuroinflammation. *Front. Immunol*. **6**, 539 (2015).
87. Alkeskas, A. et al. The molecular characterisation of Escherichia coli K1 isolated from neonatal nasogastric feeding tubes. *BMC Infect. Dis.* **15**, 449 (2015).
88. Kang, Y. J. et al. Three-dimensional human neural culture on a chip recapitulating neuroinflammation and neurodegeneration. *Nat. Protoc.* **18**, 2838–2867 (2023).

Acknowledgements

This study was funded by the National Research Foundation of Korea (NRF) grant, funded by the Korea government (MSIT) (RS-2024-00336758), the Korea Dementia Research Project through the Korea Dementia Research Center (KDRC), funded by the Ministry of Health & Welfare and Ministry of Science and ICT, Republic of Korea (RS-2022-KH126808), and the Fourth Stage of Brain Korea 21 Project in Department of Intelligent Precision Healthcare, Sungkyunkwan University (SKKU) to H.C. and the Institute of Quantum Biophysics for PhD Fellowship to V.T.A.T. We would like to express our sincere thanks to Huyen Ngo (Department of Biophysics, Sungkyunkwan University) for technical help with IRF3 immunostaining data.

Author contributions

V.T.A.T. mainly conducted the experiments, generated figures, wrote and edited the manuscript. H.C. and L.P.L conceived the project, provided guidance, and edited the manuscript. X.Z performed experiment for Fig. S9, Z.A. edited the manuscript. All authors have read and agreed to the published version of the manuscript.

Competing interests

The authors declare no competing interests.

Additional information

Supplementary information The online version contains supplementary material available at https://doi.org/10.1038/s42003-025-07787-5.

Correspondence and requests for materials should be addressed to Luke P. Lee or Hansang Cho.

Peer review information *Communications Biology* thanks the anonymous reviewers for their contribution to the peer review of this work. Primary Handling Editors: Ibrahim Javed and Benjamin Bessieres.